The geometry of wheel-rail contact

M. Arnold*

1 Introduction

In the dynamical simulation wheel-rail systems are often modelled as mechanical multibody systems (MBS). That includes models for the *geometrical* description of wheel-rail contact and for the computation of *friction forces*. Both are closely related to the elastic deformation in the *contact area* of wheel and rail. In Section 2 the geometry of wheel-rail contact is discussed for a separate wheel with wear profile. In Section 4 we present a unified approach that describes the wheel-rail contact for both elliptical and non-elliptical contact areas. The advantages of this model are illustrated by simulation results for a rigid wheelset (Section 5).

2 Wheel-rail contact: geometrical description

The elastic deformation of wheel and rail results in a contact area between both bodies. Position, size and shape of the real contact area depend in a complicated way on the relative position of wheel and rail, on contact forces, on the velocity of the rail vehicle and on many other parameters. Most of these effects may be neglected in a pure geometrical analysis.

Let a wheel and a rail be given that are in (elastic) contact. We aim at describing this contact in terms of the *undeformed* bodies of wheel and rail that are in practice defined by *profile functions*. At first choose a vertical axis on the rail. Then lift the wheel along this axis. There is exactly one position such that wheel and rail are still in contact but would lose this contact if the wheel would be lifted furthermore. In this position there is no elastic deformation, the surfaces of wheel and rail have (at least) one *common point* (in the following we say *the* common point – if there is more than one then select the one that has maximum distance from the flange of the wheel). The common point $P^{(C)} = P^{(C)}(y, x, \varphi, \psi)$ is completely defined by the lateral shift y of the wheel w. r. t. the rail, by its longitudinal position x, by roll and yaw angle φ, ψ and by the profiles of wheel and rail. It is independent of the vertical shift z and of the actual angle of rotation around the wheel axis. In the common point the tangential planes $\mathcal{E}$ of the (undeformed) surfaces of wheel and rail coincide (otherwise the surfaces would penetrate in a neighbourhood of $P^{(C)}$).

Now we approximate the real contact area by that region of $\mathcal{E}$ where the distance between the (undeformed) surfaces of wheel and rail is less than a given parameter Δ_0. This distance is measured along the normal of $\mathcal{E}$. (Typical values of Δ_0 are some $\frac{1}{10}\,\mathrm{mm}$.) In the upper right plot of Figures 1, 2 and 3 this approximation (that we call *the* contact area) is shown for a prismatic rail and profiles S1002 (wheel) and UIC60–ORE (rail) ($\Delta_0 = 0(25)150\,\mu\mathrm{m}$). The abszissa s (in m) corresponds to the direction of wheel axis ($s > -35\,\mathrm{mm}$: tread, $s < -35\,\mathrm{mm}$ flange of the wheel). The contact area is symmetric w. r. t. the abszissa axis (and does not depend on x) since the rail is prismatic.

Both in theoretical investigations and in experiments with roller rigs the profiles of wheel and rail are often substantially simplified: conic wheels and prismatic rails with elliptical cross cuts are used. Then the contact area is approximately elliptical and the common point is its centre. This motivates the notations *contact point* instead of common point and *contact ellipse* instead of contact area. In the contact ellipse the ratio of the half-axis is completely defined by the curvatures of wheel and rail in the contact point (*Hertzian contact*).

For real life profiles, especially for *wear* profiles like S1002, the situation is much more complicated. Contact ellipses around the common point are shown in the middle of the right plots in Figures 1 and 3. The approximation of the contact area may be quite good (Figure 1) or very bad (Figure 3) – even for neighbouring configurations (y, φ, ψ) . Furthermore size, position and shape of the contact area change continuously in the tread of the wheel but there are discontinuities in the common point (it "jumps"),

*University of Rostock, Department of Mathematics, Postfach, D – 18051 Rostock, Germany

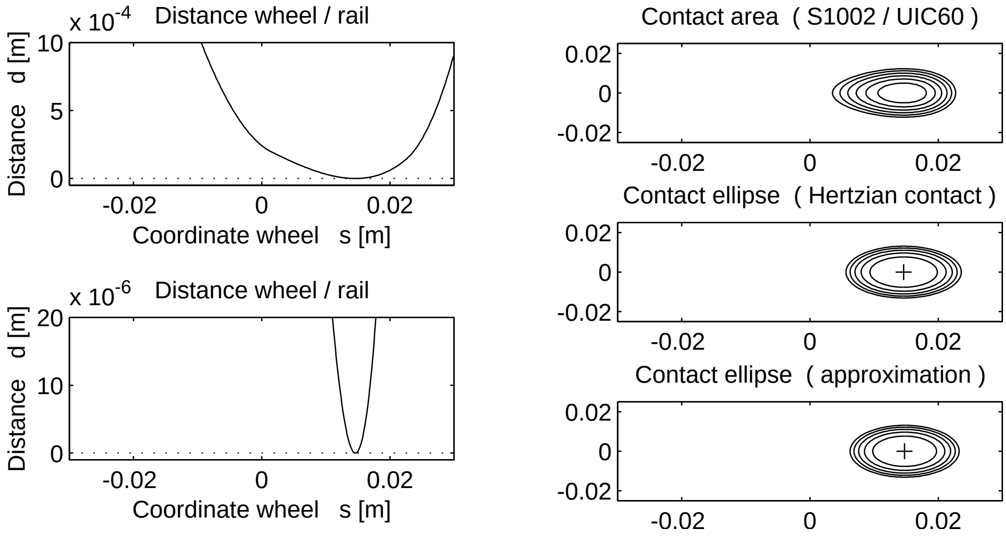

Figure 1: $y = -12.0\,\mathrm{mm}$, $\varphi = 1.0°$, $\psi = 0.0°$

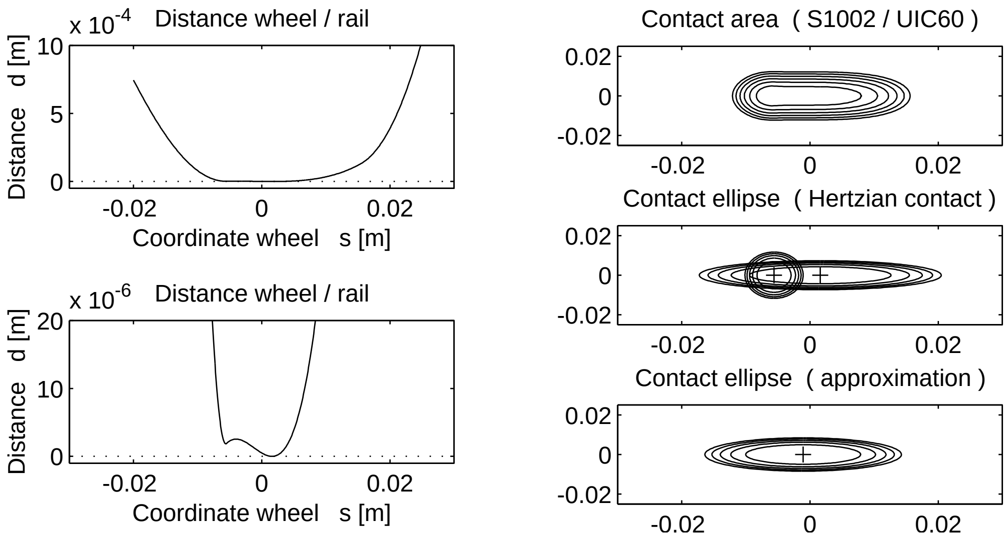

Figure 2: $y = -5.0\,\mathrm{mm}$, $\varphi = 1.0°$, $\psi = 0.0°$

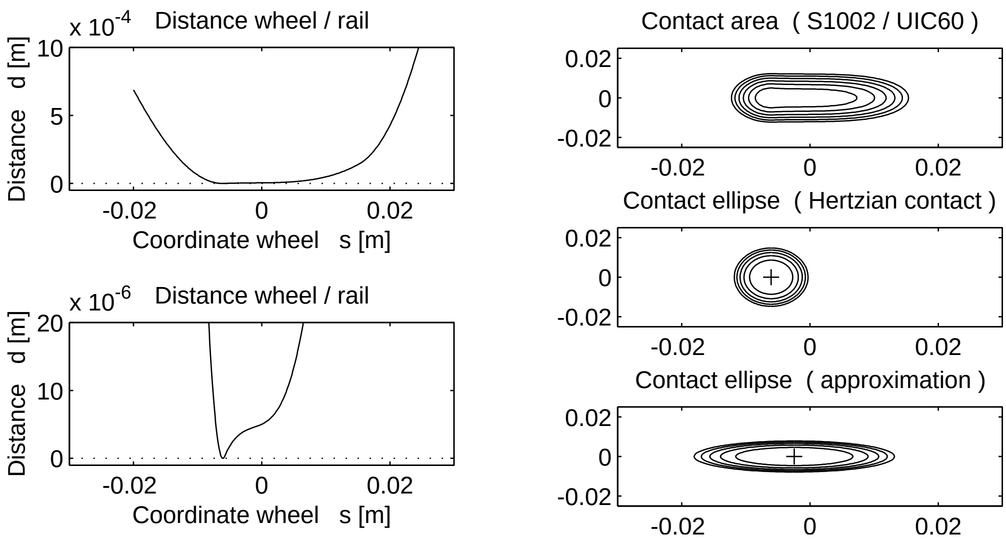

Figure 3: $y = -4.7\,\mathrm{mm}$, $\varphi = 1.0°$, $\psi = 0.0°$

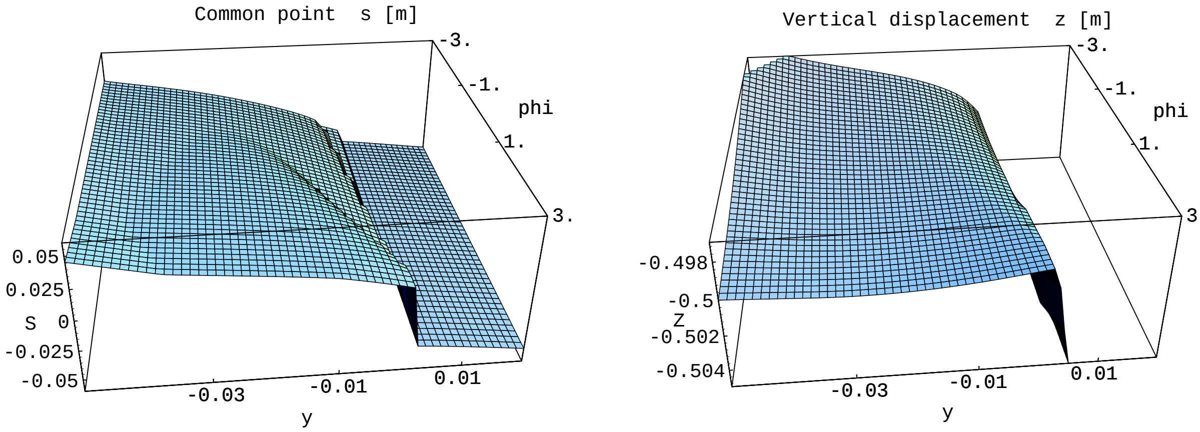

Figure 4: Common point and vertical displacement (S1002 / UIC60), $\psi = 0°$

see the left plot of Figure 4. Thus it is not surprising that the identification of common point and contact point results in large errors in simulation results (in Section 5 we refer to this model as *Hertzian one-point contact*).

3 Modifications of the Hertzian contact model

In Section 2 the common point of wheel and rail was introduced. For simplified profiles this common point gives already full information about the geometry of wheel-rail contact, this does *not* hold for wear profiles.

Nevertheless the common point will be important in the geometrical description of the contact. Thus we have to answer the question how to compute this common point: If (y, x, φ, ψ) defines the relative position of the wheel w. r. t. the rail then a function $P^{(R)}$ is introduced that maps each point $P^{(W)}$ of the (undeformed) wheel surface on the (undeformed) rail surface along the vertical axis of the rail (i. e. along the z-axis). The *distance* $\Delta(P^{(W)})$ between wheel and rail is defined by $\Delta(P^{(W)}) := \|P^{(W)} - P^{(R)}(P^{(W)})\|_2$. $P^{(W)}$ is said to be a *potential common point* if the tangential planes of wheel and rail surface in $P^{(W)}$ and $P^{(R)}(P^{(W)})$, respectively, are parallel (remember that these planes coincide in the common point if there is no elastic deformation).

Among the potential common points *the* common point is that with minimum distance Δ. This formulation

- is independent of the vertical displacement z and thus also independent of the elastic deformation and
- avoids the global search for the minimum of Δ on the (2D) wheel surface.

For conic wheels and prismatic rails with elliptical cross cuts there is exactly one potential common point for given (y, φ, ψ) , for profiles S1002/UIC60 the number of potential common points depends on (y, φ, ψ) : up to 7 potential common points are possible.

The common point is computed efficiently by a combination of bisection and Newton's method ([NA93]), small changes of its position during integration can be handled by a differential-algebraic systems solver ([SFR91], [AN93]).

For prismatic rails the normal vectors to the rail surface are in the cutting plane of the rail. I. e. all potential common points belong to the curve $\mathcal{C}$ of points on the wheel surface for that the normal vector to the wheel surface lies in such a cutting plane. The distance function Δ along $\mathcal{C}$ gives already a rough estimate of position and size of the contact area (see the left plots of Figures 1, 2 and 3, the upper one with $\Delta \in [\,0\,\mathrm{mm}, 1\,\mathrm{mm}\,]$, the lower one with $\Delta \in [\,0\,\mu\mathrm{m}, 20\,\mu\mathrm{m}\,]$). In potential common points the partial derivative $\frac{\partial}{\partial s}\Delta$ vanishes ([NA93]). In Figures 1 and 3 the common point is the only potential common point, in Figure 2 there are three potential common points.

Potential common points and the common point itself allow generalizations of the Hertzian one-point contact model for wheels with wear profiles.

A quite simple approach is the *interpolated* Hertzian contact model (that is implemented in the simulation package MEDYNA, [N94]): a set of interpolating points $(y_i, x_i, \varphi_i, \psi_i)$, $(i = 1, \ldots, N)$ is defined. In each point $(y_i, x_i, \varphi_i, \psi_i)$ the contact is modelled as Hertzian one-point contact. The parameters that define the contact ellipse (contact point, ratio of the half-axis) are interpolated e. g. by linear interpolation or by cubic splines. This avoids jumps of the contact point (even if the common point is discontinuous). But a satisfactory approximation of the real contact geometry would require a large number N of interpolation points, and then the problems of the Hertzian one-point model are reproduced: this is illustrated by an interpolation between the configurations $(-5.0\,\mathrm{mm}, 1^\circ, 0^\circ)$ and $(-4.7\,\mathrm{mm}, 1^\circ, 0^\circ)$ in Figures 2 and 3. In any case this contact model yields large errors in the dynamical simulation.

A more sophisticated approach is motivated by Figure 2. The contact area is approximated by a composition of contact ellipses around all *potential* common points that correspond to a (local) minimum of the distance function Δ. As in the Hertzian contact model the ratios of the half-axis are defined by the curvatures of wheel and rail surface. This motivates the notation *Hertzian two-point* – or in general – *Hertzian multi-point contact* (see e. g. [JS94]). To divide the reaction forces among the contact ellipses the contact is modelled elastically. This results in solutions with oscillations of high frequency and in a large amount of computing time during integration. But the main drawback of this approach is illustrated in Figure 3: in this configuration the multi-point contact coincides with the one-point contact model since there is only one potential common point. Thus the geometrical contact is modelled in completely different ways for neighbouring configurations like Figures 2 and 3. While Hertzian two-point contact gives a good approximation if the real contact area is splitted in one part on the flange and the other part on the tread of the wheel the approximation of non-Hertzian contact areas on the tread might be poor (Figure 3).

4 A unified geometrical description

In this section the point of view of *dynamical simulation* is introduced in the geometry of wheel-rail contact. In contrast to the interpolated and the multi-point Hertzian contact the contact is not considered for a single configuration of wheel and rail or for a (small) set of interpolating points. We aim at describing the geometrical contact for *all* possible configurations such that the discontinuities (or very fast changes) in the model correspond to the discontinuities of the physical phenomenon. This is illustrated in Figure 4 for wear profiles. There are discontinuities in the velocity vector and in the reaction forces when the flange of the wheel gets in contact with the rail (at $y = 0.002\,\mathrm{m}$), the common point "jumps" from tread to flange, the vertical displacement z decreases rapidly. The state changes continuously if the contact area is on the tread of the wheel, this is nicely illustrated by the right plot of Figure 4 ($y < 0.002\,\mathrm{m}$). The geometrical model of the contact should not suffer from the "jumps" of the common point within the tread that can be seen as two folds in the region $y < 0.002\,\mathrm{m}$ of the left plot in Figure 4.

In the following we consider configurations (y, x, φ, ψ) of wheel and rail such that the state of the wheel-rail system changes continuously: contact at the tread of a wheel with wear profile and arbitrary configurations for conic wheels and prismatic rails with elliptical cross cuts. Let (continuous or discontinuous) functions $\underline{f} = (f_j(y, x, \varphi, \psi))_{j=1}^{M}$ be given that approximate the geometrical parameters of the contact for a *fixed* configuration (y, x, φ, ψ) . These functions define e. g.

- the position of the common point, the vertical displacement and parameters in the model for friction forces in a rigid contact model or
- the position of the common point and the ratio of the half-axis in the contact ellipse for a (classical) elastic Hertzian contact model.

The functions $\underline{f}$ are approximated by *sufficiently smooth* functions $\Phi \in X$ such that

$$\int_\Omega \omega(y, x, \varphi, \psi)(f_j(y, x, \varphi, \psi) - \Phi_j(y, x, \varphi, \psi))^2 \, dy \, dx \, d\varphi \, d\psi \longrightarrow \min \quad , \quad j = 1, \ldots, M \tag{1}$$

$(\Omega := [\underline{y}, \overline{y}] \times [\underline{x}, \overline{x}] \times [\underline{\varphi}, \overline{\varphi}] \times [\underline{\psi}, \overline{\psi}]$). Here ω denotes a (positive) *weight function*.

From the point of view of dynamical simulation the functions in X should be (at least) continuously differentiable. Approximations to the vertical displacement z in a rigid contact model have to be two times continuously differentiable to guarantee that the reaction forces (that include the second derivatives of z w. r. t. (y, x, φ, ψ)) remain continuously. If the functions $\underline{f}$ are defined neglecting the elastic deformation (e. g. by Hertzian one-point contact) then the approximation (1) gives some "natural" smoothing of the model parameters and a generalization of the Hertzian one-point contact model to wheels with wear

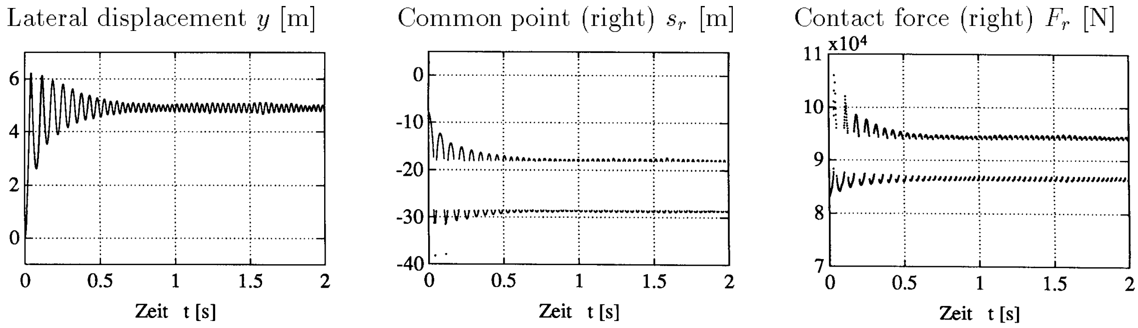

Figure 5: Motion of a rigid wheelset: Hertzian one-point contact

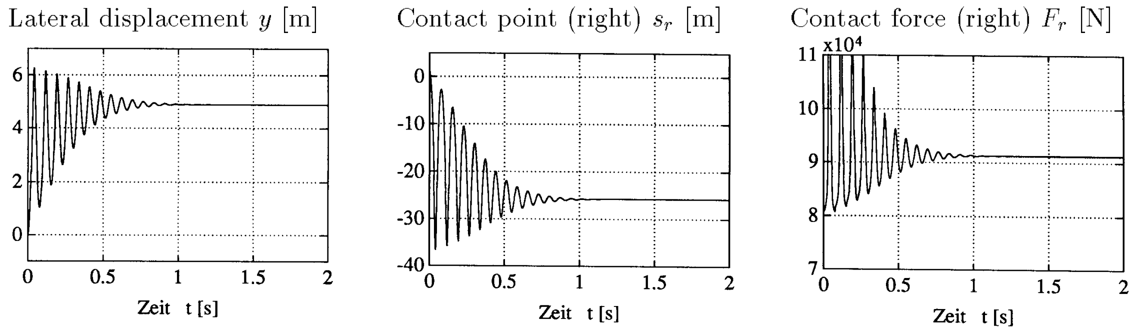

Figure 6: Motion of a rigid wheelset: approximative contact model

profiles. This motivates the notations *contact point* for the approximation of the common point and *contact ellipse* for an ellipse with ratio AB of the half-axis and the common point as centre. Here AB denotes the least-squares approximation (1) of the ratio a/b of half-axis in the Hertzian one-point contact (a/b is defined by the curvatures of wheel and rail surface in the common point).

There are various choices of the set X of functions: [FH94] discuss approximations with functions that are infinitely differentiable ($\omega \equiv 1$). We prefer the approximation with polynomial tensor product splines, then (1) reduces to a *linear* least-squares-problem that can be solved efficiently ([A94a]). This approach is implemented as (public domain) FORTRAN package **W**heel–**R**ail–**Spl**ine ([A94b], see also Section 5). The weight ω is chosen large in regions where the functions $\underline{f}$ give a good approximation of the "real" contact and small in regions where this approximation is poor (e. g. in the neighbourhood of "jumps" of the common point). These splines approximate the continuous parameters f_j very good even for coarse grids: the error in the vertical displacement z is e. g. less than $0.5\,\mathrm{mm}$ for a $10 \times 2 \times 2$ – grid in (y, φ, ψ) , the plot coincides with the original data in the right hand side of Figure 4. The corresponding approximations of the contact area are shown in the last plot at the right hand side of Figures 1, 2 and 3. Position, shape and size of the "real" contact area are reproduced.

5 Numerical Tests

The new approach to the geometrical description of wheel-rail contact was tested at various examples. In this section results for a benchmark of [PS91] are given. A rigid wheelset (S1002) is moved with constant speed along a straight track (UIC60–ORE). Besides a vertical force $F_z = 154715\,\mathrm{N}$ a force $F_y = 20000\,\mathrm{N}$ acts in lateral direction (for details see also [NA93], $\mu = 0.01$). With these settings a quasi-steady state is reached, i. e. lateral and vertical displacement, roll and yaw angle tend to finite limits for $t \to \infty$. At the right wheel a configuration similar to that of Figures 2 and 3 is reached, i. e. the error in the Hertzian one-point contact model is quite large. This yields to large errors in the simulation results (Figure 5). The numerical solution has many discontinuities in the velocity vector and the reaction forces because of jumps in the common point, no quasi-steady state is reached.

The advantages of the spline approximation (Figure 6) are obvious. We used quadratic interpolation w. r. t. ψ and cubic tensor product splines w. r. t. (y, φ) on a 15×4 – grid to approximate the contact area by a contact ellipse (see Section 4). The friction forces were computed by Kalker's theory of rolling contact (program FASTSIM, [Kal82]); all input parameters that depend on the curvature of the surfaces of wheel and rail in the contact point are approximated in the same way as the contact point. Note, that there is no theoretical justification of this application of FASTSIM. It is motivated both by the good approximation of the contact area in Figures 1, 2 and 3 and by the simulation results. In contrast to the Hertzian one-point contact model there is now a time-consuming pre-processing for the computation of the spline coefficients (up to 50% of the computing time for one simulation like that of Figures 5 and 6). But this pre-processing is necessary only once for given profiles of wheel and rail. The computing time for the simulation is reduced to less than 30% in this benchmark since the time-consuming re-initializations of the integrator at discontinuities are avoided.

Summary

The unified approach to the geometrical description of wheel-rail contact generalizes the Hertzian one-point contact to wheels with wear profiles. In combination with a spline approximation and the program FASTSIM for the computation of the friction forces an algorithm is obtained that allows to simulate the dynamical behaviour of wheel-rail systems correctly and with a small amount of computing time. It should be pointed out that this approach is useful also in combination with more complicated models for the computation of the friction forces and with elastic models of rolling contact.

Acknowledgement

I would like to thank Dipl.-Ing. H. Netter (DLR Oberpfaffenhofen) for many interesting discussions and helpful remarks concerning the topic of the present paper. Furthermore he carried out the experiments that are shown in Section 5.

References

[AN93] M. Arnold and H. Netter. Ein modifizierter Korrektor für die stabilisierte Integration differential-algebraischer Systeme mit von Hessenbergform abweichender Struktur. Technical Report IB 515–93–03, DLR, D-5000 Köln 90, 1993.

[A94a] M. Arnold. The computation of an approximating polynomial 2D tensor product spline. *in preparation*, 1994.

[A94b] M. Arnold. Wheel–Rail–Spline. Documentation, University of Rostock, Department of Mathematics, 1994.

[FH94] K. Frischmuth and M. Hänler. (NN). These proceedings.

[JS94] J.Ch. Jensen and E. Slivsgaard. Modelling of railway vehicles using elastic contact and moveable track. These proceedings.

[Kal82] J.J. Kalker. A fast algorithm for the simplified theory of rolling contact. *Vehicle Systems Dynamics*, 11:1–13, 1982.

[NA93] H. Netter and M. Arnold. Geometrie und Dynamik eines Rad-Schiene-Modells in Deskriptorform mit unstetigen Zustandsgrößen. Technical Report IB 515–93–02, DLR, D-5000 Köln 90, 1993.

[N94] H. Netter. MKS–Simulation von Schienenfahrzeugen: Konzeption in SIMPACK. These proceedings.

[PS91] J.P. Pascal and G. Sauvage. New method for reducing the multicontact wheel/rail problem to one equivalent rigid contact patch. In *The Dynamics of Vehicles on Roads and on Railway Tracks, 12th IAVSD–Symposium Lyon*, pages 475–489. Swets & Zeitlinger, B.V. Lisse, 1991.

[SFR91] B. Simeon, C. Führer, and P. Rentrop. Differential-algebraic equations in vehicle system dynamics. *Surveys on Mathematics for Industry*, 1:1–37, 1991.